

Isotope shift of the 590-cm^{-1} Raman feature in underdoped $\text{Bi}_2\text{Sr}_2\text{CaCu}_2\text{O}_{8+\delta}$

K. C. Hewitt, N. L. Wang, and J. C. Irwin

Department of Physics, Simon Fraser University, Burnaby, British Columbia, Canada V5A 1S6

D. M. Pooke

Industrial Research Limited, P. O. Box 31310, Lower Hutt, New Zealand

A. E. Pantoja and H. J. Trodahl

School of Chemical and Physical Sciences, Victoria University of Wellington, P. O. Box 600, Wellington, New Zealand

(Received 16 February 1999)

Raman-scattering studies have been performed on underdoped $\text{Bi}_2\text{Sr}_2\text{CaCu}_2\text{O}_{8+\delta}$. In single crystals underdoped by oxygen removal, a 590-cm^{-1} peak is observed in the B_{1g} spectrum. The feature is observed to soften in frequency by 3.8% with isotopic exchange of ^{16}O by ^{18}O . In contrast, the 590-cm^{-1} peak is not observed in crystals underdoped by Y substitution which suggests that it is a vibrational mode activated by oxygen deficiency. We have also found that underdoping leads to a depletion of low-energy spectral weight from regions of the Fermi surface located near the Brillouin-zone axes. [S0163-1829(99)51238-1]

One of the interesting electronic properties of underdoped high-temperature cuprate superconductors is the presence of a normal-state pseudogap (PG) that appears¹ at a temperature T^* which is well above the superconducting transition temperature T_c . Evidence for this electronic gaplike feature has been obtained using many different experimental techniques.¹ In particular, angle-resolved photoemission spectroscopy (ARPES)²⁻⁴ and electronic Raman-scattering (ERS) spectroscopy⁵⁻⁷ measurements have provided direct evidence of a spectral weight depletion from regions of the Fermi surface near $(\pi,0)$ in underdoped cuprates. Raman-scattering experiments have also been used⁸⁻¹² to probe the energy scale and temperature dependence of the pseudogap.

Theories of the cuprate pseudogap can be separated into two broad categories.¹³ First there are those^{14,15} that associate the PG with some form of precursor superconductivity. In this case uncorrelated pairs can form at $T > T_c$, with phase coherence and hence superconductivity occurring at T_c . The magnitudes of the PG (E_g) and superconducting gap [$\Delta(k)$] should thus be equal, and furthermore they should have the same symmetry. Thus there should be a smooth evolution from PG to superconducting gap (SCG) as the temperature is lowered through T_c . In a second category of theories the loss of spectral weight associated with the PG is attributed to short-range magnetic correlations,^{16,17} or magnetic pairing of some sort.^{18,19} In this case the magnitude of the PG should be determined by the antiferromagnetic exchange energy J , which in the cuprates is much larger than $\Delta(k)$.

Both ERS and ARPES have produced¹ similar results for the magnitude ($2\Delta_{max} \approx 8k_B T_c$) and symmetry ($d_{x^2-y^2}$) of the superconducting gap in optimally doped cuprates. In underdoped materials, ARPES measurements¹⁻⁴ on $\text{Bi}_2\text{Sr}_2\text{CaCu}_2\text{O}_{8+\delta}$ (Bi2212) suggest that the pseudogap evolves continuously into the SCG and thus has magnitude $E_g \approx \Delta$ and $d_{x^2-y^2}$ symmetry. The ARPES results are supported by the Raman measurements of Blumberg *et al.*^{11,12} who attributed a weak peak, with frequency $\omega \approx 600\text{ cm}^{-1}$ in the B_{1g} spectrum of underdoped Bi2212 to the formation

of a bound state, associated with precursor pairing of quasiparticles above T_c . However, these results are in direct contrast to other Raman studies⁵⁻⁹ which conclude that the pseudogap does not have $d_{x^2-y^2}$ symmetry and has a magnitude $E_g \approx J \approx 100\text{ meV} > \Delta$, where J is the antiferromagnetic exchange constant.

Given the potential significance of the peak near 600 cm^{-1} we sought to determine whether the excitation was affected by ^{18}O substitution. We have carried out experiments on two pairs ($T_c = 51\text{ K} - 51\text{ K}$, $82\text{ K} - 85\text{ K}$) of underdoped samples of Bi2212, one containing the ^{18}O isotope and the other ^{16}O . While confirming the expected shift of previously identified oxygen-related phonons we have also found that the 590-cm^{-1} B_{1g} mode shifts with ^{18}O substitution. This result, combined with experiments on Y-doped Bi2212 have led us to conclude that the 590-cm^{-1} mode is more appropriately assigned to an oxygen deficiency related vibration.

Through oxygen exchange methods ^{16}O and ^{18}O single crystals of Bi2212 were prepared with similar T_c 's in the underdoped regime. Fully exchanged and underdoped ^{18}O samples were prepared by completing the following steps. A sample of ^{16}O -Bi2212 was first annealed in vacuum at 500°C for four hours. The ampoule containing the sample was then evacuated again and backfilled with ^{18}O to a pressure of less than 1 atm. The sample was then annealed in the ^{18}O atmosphere for 24 h at 850°C after which it was gradually cooled over a period of 15 h to a temperature of 300°C . Then oxygen was unloaded by the following procedure. The ampoule was evacuated, then annealed at 500°C , then cooled to 350°C and quenched to room temperature. The ^{18}O samples exhibited a magnetically determined superconducting onset temperature of 51 K. An unexchanged sample, ^{16}O Bi2212, was also prepared using the same final unloading anneal, and exhibited a superconducting onset temperature of 51 K.

The second method of underdoping relies on the use of cation substitution methods. In this case the substitution of

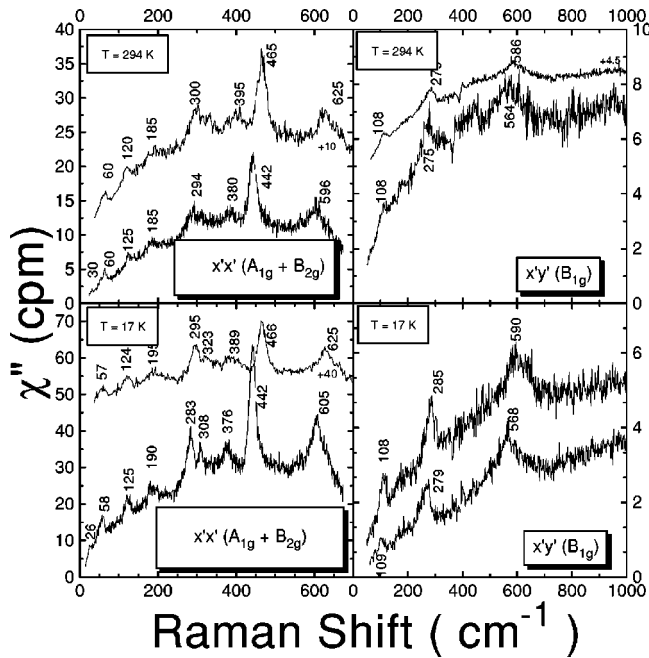


FIG. 1. The Raman spectra of ^{18}O exchanged (lower curve in each panel) and unexchanged ^{16}O (upper curve in each panel) Bi2212, taken at 294 and 17 K in the $x'x'$ ($A_{1g} + B_{2g}$) and $x'y'$ (B_{1g}) geometry. Both ^{18}O and ^{16}O crystals have $T_c \approx 51$ K and $\lambda_{\text{laser}} = 514.5$ nm, but similar spectra was obtained with the 488.0 excitation.

trivalent yttrium (Y^{3+}) for divalent calcium (Ca^{2+}) reduces the hole concentration in Bi2212. Adding Y causes T_c to fall,²⁰ and yields a nonsuperconducting compound at a Y content of 0.50.²¹ Single crystals of Y-doped Bi2212 were prepared as described elsewhere.²⁰ In the crystals studied, electron dispersive x-ray (EDX) analysis revealed a yttrium content of 0.40 and 0.07, with superconducting transition temperatures of 30 and 70 K, respectively.

Raman vibrational spectra in the frequency range 20–1000 cm^{-1} were obtained using the 514.5 and 488.0 nm lines of an argon ion (Ar^+) laser as the excitation source. The Raman measurements were carried out in a quasiback-scattering geometry, with the incident laser beam directed perpendicular to the freshly cleaved (a, b) face of the crystal.

Bi2212 has an orthorhombic structure with the a and b axes oriented at 45° to the Cu-O bonds. In Raman experiments it is customary to assume a tetragonal structure with axes parallel to a and b . To facilitate comparison with other cuprates, however, we will consider a tetragonal cell with x and y axes parallel to the Cu-O bonds. Another set of axes, x' and y' are rotated by 45° with respect to the Cu-O bonds. The $x'y'$ (B_{1g}) scattering geometry means that the incident (scattered) light is polarized along x' (y') and selection of this scattering channel enables coupling to excitations having B_{1g} symmetry. Similarly, the xy geometry allows coupling to B_{2g} excitations, which transforms as d_{xy} . Finally, the diagonal scattering geometry $x'x'$ allows coupling to $A_{1g} + B_{2g}$ and xx to $A_{1g} + B_{1g}$ excitations. Thus, by choosing the polarization of the incident and scattered light one may select different components of the Raman tensor and thus various symmetry properties of the excitations.

Figure 1 shows the B_{1g} ($x'y'$) and ($A_{1g} + B_{2g}$) ($x'x'$)

Raman response functions of the underdoped ^{18}O and ^{16}O crystal, taken at room temperature and at $T = 17$ K. The observed spectral features may be separated into two categories, modes unaffected by ^{18}O substitution and modes softened by ^{18}O substitution. The low-frequency ($\omega < 200$ cm^{-1}) modes are unaffected by ^{18}O substitution while modes above this frequency show a decrease in frequency. The heavy metal ion (BiSr) modes have low frequencies and, consistent with our observation, should be unaffected by ^{18}O substitution.

In the B_{1g} geometry, the 285-cm^{-1} mode shows a softening of 2.1% while the low frequency mode at 108 cm^{-1} shows no shift at all, consistent with the results of other isotope studies.^{22,23} The 285-cm^{-1} mode has been assigned to out-of-phase vibrations of oxygens in the CuO_2 plane, while the 108-cm^{-1} mode has been assigned to b -axis vibrations of Bi^{24} .

With ^{18}O exchange the 590-cm^{-1} feature observed in B_{1g} softens in frequency by 3.8%, from 590 to 568 cm^{-1} (see Fig. 1). Also, relative to the continuous background, the intensity of the feature increases with decreasing temperature. Identical results were obtained for the frequencies and isotope shift in the second pair ($T_c = 82, 85$ K) of underdoped crystals (see Fig. 2).

Since the 590-cm^{-1} B_{1g} feature is only observed in underdoped crystals, and since the mass dependence is consistent with an oxygen related vibration, we sought to determine whether underdoping without a corresponding reduction in δ affects the properties of the mode. This was achieved by substitution of Y^{3+} for Ca^{2+} . As shown in Fig. 3, for a $[\text{Y}] = 0.4$ and 0.07 , the 590-cm^{-1} mode is com-

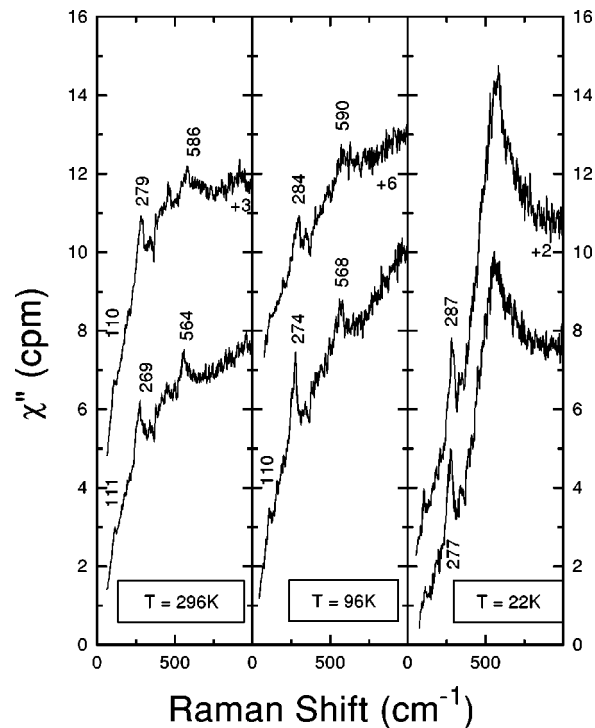


FIG. 2. The Raman spectra of ^{18}O exchanged (lower curve in each panel) and unexchanged ^{16}O (upper curve in each panel) Bi2212, taken at 294, 96 and 22 K in the $x'y'$ (B_{1g}) geometry. The ^{18}O and ^{16}O crystals have T_c of 82 and 85 K, respectively. The curves have been shifted for clarity.

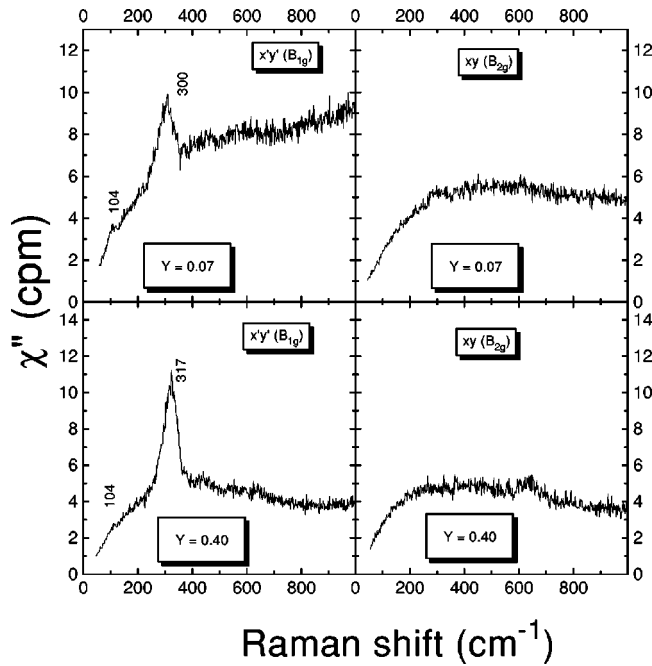


FIG. 3. The Raman spectra of Y-doped Bi2212 with $Y=0.07$ (upper panels) and $Y=0.40$ (lower panels), taken at 294 K in the $x'y'$ (B_{1g}) and xy (B_{2g}) geometry.

pletely absent from the B_{1g} spectra, as found by Kendziora²⁵ for two other underdoped crystals ($[Y] = 0.12, 0.15$). This result implies that the 590-cm^{-1} B_{1g} mode is associated with oxygen removal, and is thus expected to be related to an oxygen deficiency type of vibration. In this regard it should be noted that we do not expect the 590-cm^{-1} mode to necessarily be absent in spectra obtained from all Y-substituted samples, but only from those that are fully oxygenated.

To speculate on the origin of the 590-cm^{-1} mode one can first note that there appears to be an analogous situation in Y123. In Y123, a mode appears^{26,27} in the B_{1g} channel at about 600 cm^{-1} when the oxygen concentration is reduced below its optimum value of $x \approx 6.95$. In this case underdoping is associated with oxygen removal from the chains and the creation of chain fragments. Thus many oxygen atoms in the chains are no longer situated at centers of inversion and previously forbidden modes can become Raman active. In the case of Bi2212 one can note that the Bi-O layers are weakly bonded to one another and oxygen intercalation or exchange takes place in these planes.^{23,28} There is also an incommensurate structural modulation along the b axis in the Bi-O planes²⁸ that results from oxygen nonstoichiometry and a lattice mismatch between the Bi-O rocksalt layers and the perovskite layers. The removal of oxygen from Bi2212 should thus give rise to the formation of buckled Bi-O modulation chain fragments, and hence to disorder that would lead to the activation of normally Raman forbidden modes. Thus one might speculate that the 590-cm^{-1} mode in Bi2212 results from b -axis stretching vibrations of oxygen atoms in the Bi-O layer. The buckling associated with the modulation could lead to a broadening of the mode, consistent with observation.

In previous experiments on Y123 (Ref. 6) and La214 (Ref. 7) it was found that underdoping led to a reduction of the scattering intensity in the B_{1g} channel. In other words,

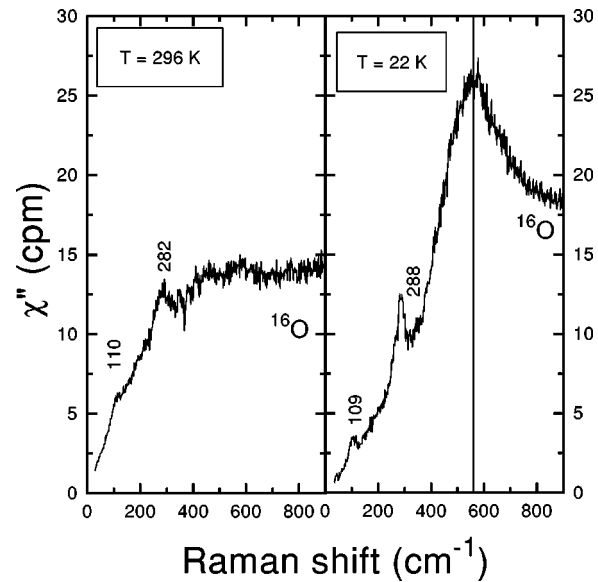


FIG. 4. The Raman spectra of optimally doped ^{16}O Bi2212 ($T_c=90\text{ K}$), taken at 296 and 22 K in the $x'y'$ (B_{1g}) geometry.

spectral weight was lost from regions of the Fermi surface located near $(\pi,0)$ and symmetry related points. The present spectra suggest that a similar depletion occurs in underdoped Bi2212.

In the optimally doped material (Fig. 4) the continuum in the B_{1g} spectrum is characterized by a count rate per minute of approximately 15 cpm ($T=296\text{ K}$) and a strong superconductivity induced renormalization is observed when the sample is cooled through T_c .

In the underdoped compound with $T_c=51\text{ K}$ the strength of the B_{1g} spectrum is reduced to about 4 cpm (Fig. 1). In the Y substituted compounds (Fig. 3), for the sample with $[Y]=0.07$ ($T_c \approx 70\text{ K}$), $\chi''(B_{1g}) \approx 9\text{ cpm}$ and for $[Y]=0.4$ ($T_c \approx 30\text{ K}$) one has $\chi''(B_{1g}) \approx 4\text{ cpm}$. One can also note that there is no B_{1g} renormalization at T_c for the underdoped compounds.

In the B_{2g} channel the strength of the spectrum (Fig. 3) is approximately the same for both Y-doped compounds and is

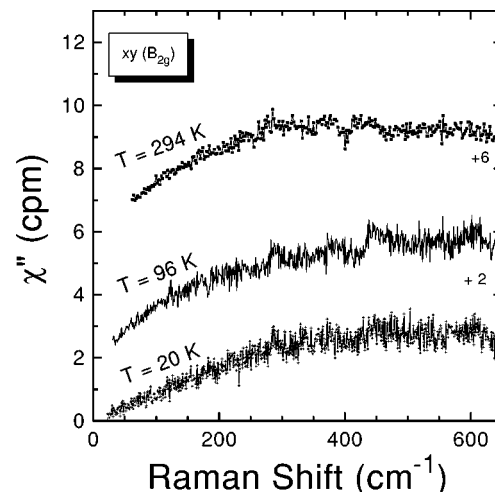


FIG. 5. The Raman spectra of ^{18}O exchanged Bi2212 ($T_c=51\text{ K}$), taken at three temperatures (294, 96, and 20 K) in the xy (B_{2g}) scattering geometry.

given by $\chi''(B_{2g}) \approx 4$ cpm. In the ^{18}O -Bi2212 crystal the B_{2g} spectrum (Fig. 5) also has $\chi''(B_{2g}) \approx 4$ cpm. It is interesting to note that there does not appear to be a well-defined renormalization of the B_{2g} spectrum at T_c .

We have determined the ratio $R = \chi''(B_{1g})/\chi''(B_{2g})$ for the above compounds and find that it decreases by about a factor of four as the doping level is decreased from optimum ($T_c = 90$ K) to the lowest value examined here ($T_c = 40$ K). A corresponding hole concentration can be estimated²⁹ from $T_c/T_{c,max} = 1 - 82.6(p - p_{opt})^2$. The magnitude and rate of decrease in R is similar to the Bi2212 results of Opel *et al.*⁹ and to values found for Y123 (Ref. 6) and La214.⁷ Since $\chi''(B_{2g})$ is approximately independent of doping, the decrease in R is attributed to a depletion of spectral weight in the B_{1g} channel.

Since the decrease in strength of the Bi2212 B_{1g} spectrum with decreasing doping is similar to that observed in Y123 and La214, we suggest that the depletion of B_{1g} spectral weight in underdoped compounds is a characteristic feature of the cuprates. The depletion is attributed^{6,7} to the existence of a pseudogap of magnitude $E_g \approx J$ that is localized near $(\pi, 0)$. As the doping level is decreased more and more of the Fermi surface becomes depleted. Or, from another per-

spective, the Fermi surface in underdoped compounds appears to consist of arcs centered near the diagonal directions in k space. Our results thus suggest that the lengths of the arcs decrease with decreasing doping⁷. One can also see (Fig. 1) that, at low energies, $\chi''(B_{1g})$ decreases with temperature, as observed¹⁰ previously in Bi2212.

In conclusion, the 590-cm^{-1} B_{1g} mode is found in the Raman spectra of Bi2212 in which underdoping is achieved by the process of oxygen depletion. This mode is absent in spectra obtained from crystals in which underdoping is achieved by cation substitution. The mode softens by 3.8% with ^{18}O substitution. Based on these observations we conclude that the 590-cm^{-1} feature is vibrational in origin and not associated with pseudogap formation. However, in this regard, underdoping of Bi2212 leads to a depletion of spectral weight from regions of the Fermi surface near $(\pi, 0)$. The strength of this depletion is consistent with that observed in other cuprates.

Financial support from the Industrial Research Limited and the Natural Sciences and Engineering Research Council of Canada is gratefully acknowledged. We would also like to thank T. P. Devereaux, R. G. Buckley, and J. L. Tallon for fruitful discussions.

-
- ¹T. Timusk and B. Statt, Rep. Prog. Phys. **62**, 61 (1999).
²D. S. Marshall *et al.*, Phys. Rev. Lett. **76**, 4841 (1996).
³J. M. Harris *et al.*, Phys. Rev. B **54**, R15 665 (1996).
⁴H. Ding *et al.*, Nature (London) **382**, 51 (1996).
⁵X. K. Chen *et al.*, Phys. Rev. B **56**, R513 (1997).
⁶X. K. Chen *et al.*, J. Phys. Chem. Solids **59**, 1968 (1998).
⁷J. G. Naeini *et al.*, Phys. Rev. B **59**, 9642 (1999).
⁸R. Nemeschek *et al.*, Phys. Rev. Lett. **78**, 4837 (1997).
⁹M. Opel *et al.*, J. Phys. Chem. Solids **59**, 1942 (1998).
¹⁰J. W. Quilty, H. J. Trodahl, and D. M. Pooke, Phys. Rev. B **57**, R11 097 (1998).
¹¹G. Blumberg *et al.*, J. Phys. Chem. Solids **59**, 1932 (1998).
¹²G. Blumberg *et al.*, Science **278**, 1427 (1997).
¹³J. Maly, B. Janko, and K. Levin, cond-mat/9805018 (unpublished).
¹⁴V. J. Emery and S. A. Kivelson, Nature (London) **374**, 434 (1995).
¹⁵V. J. Emery, S. A. Kivelson, and O. Zachar, Phys. Rev. B **56**, 6120 (1997).
¹⁶J. M. Wheatley, T. S. Hsu, and P. W. Anderson, Phys. Rev. B **37**, 5897 (1988).
¹⁷N. Nagaosa and P. A. Lee, Phys. Rev. Lett. **64**, 2450 (1990).
¹⁸D. Pines, Physica C **282-287**, 273 (1997).
¹⁹D. Pines, Z. Phys. B: Condens. Matter **103**, 129 (1997).
²⁰N. L. Wang, B. Buschinger, C. Geibel, and F. Steglich, Phys. Rev. B **54**, 7445 (1996).
²¹M. Kakihana *et al.*, Phys. Rev. B **53**, 11 796 (1996).
²²A. A. Martin and M. J. G. Lee, Physica C **254**, 222 (1995).
²³A. E. Pantoja, D. M. Pooke, H. J. Trodahl, and J. C. Irwin, Phys. Rev. B **58**, 5219 (1998).
²⁴R. Liu, M. V. Klein, P. D. Han, and D. A. Payne, Phys. Rev. B **45**, 7392 (1992).
²⁵C. Kendziora, J. Phys. Chem. Solids **59**, 1991 (1998).
²⁶V. G. Hadjiev *et al.*, Solid State Commun. **80**, 643 (1991).
²⁷V. G. Ivanov, M. N. Iliev, and C. Thomsen, Phys. Rev. B **52**, 13 652 (1995).
²⁸S. T. Johnson, P. D. Hatton, A. J. S. Chowdury, and B. M. Wanklyn, Solid State Commun. **94**, 261 (1995).
²⁹J. L. Tallon *et al.*, Phys. Rev. B **51**, 12 911 (1995).